Ocean-Based Passive Decay Heat Removal in the Offshore Floating Nuclear Plant

Ocean-based Passive Decay Heat Removal in the Offshore Floating Nuclear Plant (OFNP)

J. Zhang, J. Buongiorno*, M. Golay, N. Todreas
Nuclear Science and Engineering Department, Massachusetts Institute of Technology
Cambridge MA, 02139
jacopo@mit.edu

ABSTRACT

The Offshore Floating Nuclear Plant (OFNP) concept offers the potential for superior economics and safety. The 300 MWe version of the OFNP features an integral primary system PWR, and adopts an ocean-based direct reactor auxiliary cooling system (DRACS) which provides passive and indefinite decay-heat removal from the reactor pressure vessel during abnormal occurrences without primary system depressurization, e.g. a loss of flow accident. In this paper we present analyses aimed at sizing and evaluating the performance of the DRACS loops and heat exchangers, to ensure adequate core cooling and a compact layout. We assume that all the residual heat is removed by the DRACS for the condition that the reactor coolant pumps have stopped and thus the system operates in natural circulation mode. The DRACS effectively consists of three coupled flow loops: first, natural circulation in the primary system from the core to the core makeup tank (CMT); second, natural circulation from the CMT to the ultimate heat exchanger; third, natural convection of seawater in the shell of the ultimate heat exchanger. The asymptotic (quasi-steady) behavior of these loops was first modeled using hand calculations, which allowed estimation of the size of the heat exchangers. Then a transient analysis of this preliminary design was performed with the code RELAP5, to confirm that the principal safety margins (margin to boiling, MDNBR, and maximum allowable reactor coolant pressure) are not challenged.

KEYWORDS
Offshore Floating Nuclear Plant (OFNP), direct reactor auxiliary cooling system (DRACS), core makeup tank (CMT), ultimate heat exchanger, natural circulation

1. INTRODUCTION

The Offshore Floating Nuclear Plant (OFNP) concept combines two mature and successful technologies, i.e., LWRs and floating platforms of the type used in offshore oil/gas operations, each with an established and cost-effective global supply chain [1]. OFNP is a plant that can be entirely built within a floating platform in a shipyard, transported to the site, where it can be moored within a dozen miles off the coast, within territorial waters, and connected to the grid via submarine transmission cables. The OFNP can achieve excellent economics through plant simplification, modularity and shipyard construction and efficient decommissioning. Two OFNP designs are being developed in parallel, to be used in different markets: the OFNP-300 and OFNP-1100, designated according to their electric power rating. In this paper we focus on the OFNP-300, shown in Figure 1. The OFNP-300 could be based on a class 300 MWe reactor, such as Westinghouse's Small Modular Reactor (WSMR) [2-5]. The floating structure chosen to house the nuclear plant is a cylindrical-hull platform that shares many of its characteristics with platforms used in the offshore oil and gas drilling industry. Cylindrical platforms offer superior hydrostatic and hydrodynamic stability at the scale the OFNP is designed for [6], as well excellent protection to the reactor itself when compared to other offshore platform designs, such as semi-submersibles or floating barges. Locating the reactor in a center annulus offers it substantial physical

protection via multiple hulls. Additionally, the cylindrical hull design enables the reactor and containment to be located at an elevation below the waterline, which enhances physical protection from plane crashes and collisions with ships, in addition making it easier to access the ocean heat sink. Overall, the cylindrical hull platform affords a more vertical plant organization than alternative platform designs or existing terrestrial plants, which makes the entire design more compact. Summary dimensions for the OFNP-300 platform are reported in Table I. More information about both the OFNP-300 and OFNP-1100 designs can be found in Ref. [1]. Since the OFNP is a floating plant, seismic loads from the ocean floor do not transfer to the plant structures; consequently, earthquakes are eliminated as a safety concern. Moreover, the plant is sited within a dozen miles off the coast, where tsunami waves are much smaller and their wavelength so long (i.e., order of tens of kilometers) that, upon passage of a tsunami wave, the plant simply rides the wave without danger of being submerged. Therefore, tsunamis are also eliminated as accident precursors. Of course severe storms are a concern. However, the platform can be designed to withstand extreme storms (e.g., Category 5 hurricanes) and be sited preferentially in regions with low storm frequency and intensity.

Table I. OFNP platform characteristics

Parameter	OFNP-300
Hull /skirt diameter (m)	45/75
Draft (m)	49
Total height (m)	73
Main deck height (m)	12
Displacement (tons)	~72, 000
Natural period for heave/pitch (s)	~21/23

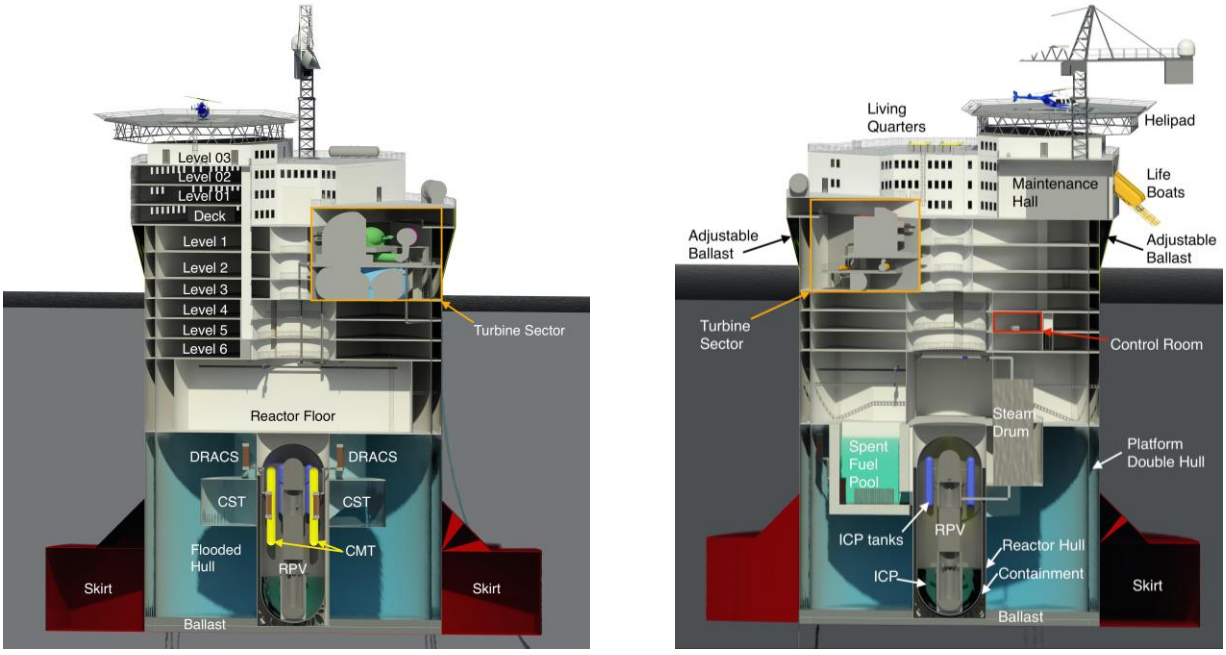

Figure 1. Isometric views of OFNP-300

2. SAFETY SYSTEMS

The OFNP safety case is based on a four-pronged strategy: (i) minimize accident precursors (especially external events) by design, (ii) use passive safety systems to respond to design-basis accidents and minimize the likelihood of severe (beyond-design-basis) accidents, (iii) adopt a robust containment design to cope with these accidents, and (iv) minimize on-land consequences of these accidents. While all four elements of the strategy are important, here we focus on number (ii), i.e. the passive safety systems. OFNP-300 uses an ocean-based Direct Reactor Auxiliary Cooling System (DRACS) to remove decay heat from the core passively and indefinitely during loss of feedwater or loss of offsite power events (Fig. 2). The DRACS operates indefinitely without AC power or refilling of tanks. As such, the OFNP design has eliminated the loss of ultimate heat sink accident .The Emergency Core Cooling System (ECCS) and ocean-based Passive Containment Cooling System (PCCS) maintain the fuel covered and the containment pressure low during Loss of Coolant Accidents (LOCAs) (Fig. 3a). For hypothetical severe accidents with core melting the In-Vessel Retention (IVR) approach is adopted; the containment is normally under vacuum, to prevent hydrogen explosions; the PCCS again ensures indefinite and passive heat removal through the containment shell (Fig. 3b). Note that no seawater is ever present within the containment or the pressure vessel.

In this paper we present the conceptual design and sizing of the DRACS (Section 3), and its performance during a station blackout, i.e., combined loss of flow + loss of all feedwater (Section 4).

3. SIZING OF THE DRACS

The DRACS is a natural circulation based system, employing the ocean as the ultimate heat sink Following the schematic in Fig. 4, the residual heat is transferred from the core to an intermediate closed water loop and ultimately to the sea water. There are two heat exchangers (enclosed in green circles in the figure): the first one is within the Core Makeup Tanks (CMT) between the primary loop and the intermediate closed loop of DRACS; the second one is the heat exchanger in the seawater. Hence the DRACS effectively consists of three coupled flow loops: first, natural circulation in the primary system from the core to the CMT; second, natural circulation from the CMT to the ultimate heat exchanger; third, natural convection of seawater in the shell of the ultimate heat exchanger. The DRACS heat removal capacity depends on the size and relative elevation of the heat exchangers as well as the hydraulic resistance in all three loops. In this section the DRACS size is estimated by means of hand calculations that model the asymptotic (quasi-steady) decay heat removal of the OFNP-300.

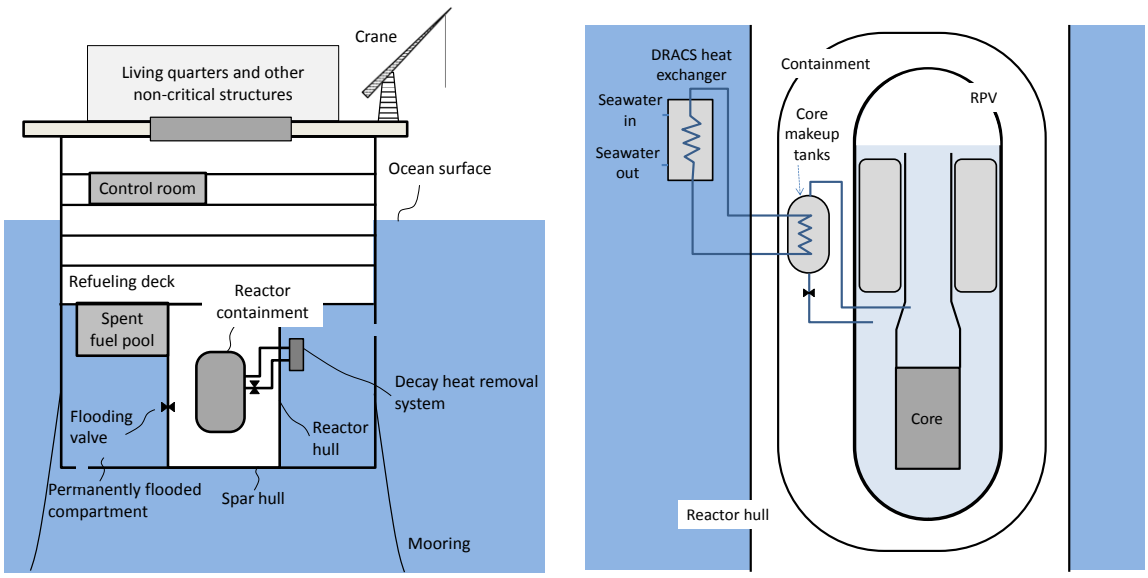

(a) (b)

Figure 2. Schematic drawings of the OFNP-300 (a) platform and (b) DRACS.

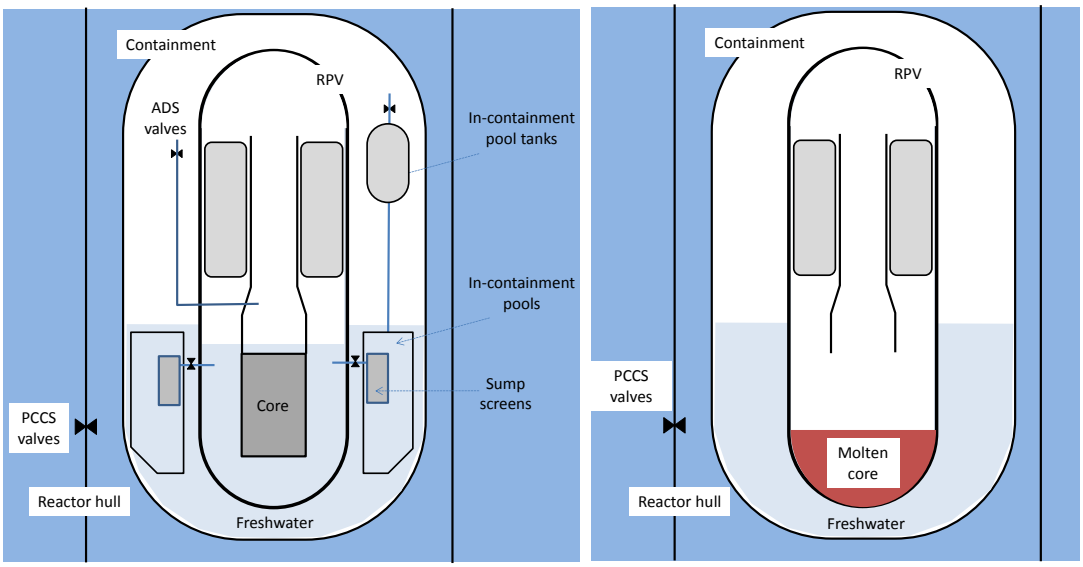

(a) (b)

Figure 3. Schematic drawings of the OFNP-300 (a) core and containment cooling in a post-LOCA situation, and (b) in-vessel retention of molten core.

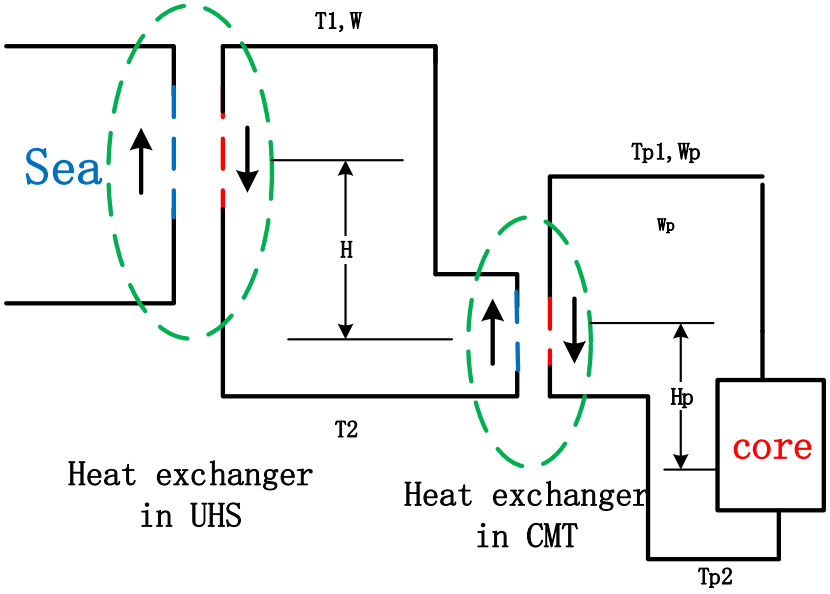

Figure 4. Schematic diagram and nomenclature of the DRACS loops

First let us assume a station blackout occurs which causes a trip of the reactor coolant pumps, a reactor trip and a complete loss of feedwater. Since the OFNP does not have safety-grade auxiliary feedwater, the only decay heat removal path is ultimately through the DRACS. Assume quasi-steady state is reached after the feedwater and main steam isolation valves are closed. This means that natural circulation in the three DRACS loops has been established and all core decay heat is removed by the DRACS. Under these conditions the DRACS behavior can be described by the following simplified analysis.
The energy conservation equation for the first loop is shown below:

$$Q_p = (T_{p1} - T_{p2}) \cdot W_p \cdot C_p , \tag{1}$$

where Q_p is the heat removed from each CMT, that is, $Q_p = Q_s / 4$, as there are four CMTs; Q_s is the total residual power generated in the core, which is assumed constant and equal to 10.3 MWt or 1.1% of the nominal core power; T_{p1} and T_{p2} are the outlet and inlet temperature of the core, respectively; W_p is the flow rate in each CMT; C_p is the average specific heat in the primary loop. The momentum conservation equation for the first loop can be written as:

$$\Delta P_p(W_p) = \Delta P_{friction}(W_p) + \Delta P_{form}(W_p) + \Delta P_{gravity}(W_p) = 0 , \tag{2}$$

where ΔP_p is the pressure drop of primary loop; $\Delta P_{friction}$ is the friction pressure drop; ΔP_{form} is the form pressure drop; $\Delta P_{gravity}$ is the gravity pressure drop, which acts as the driving head for natural circulation and depends on the coolant density and height difference: a linear density change is assumed along the core and the CMT heat exchanger, expressed as $\rho_p g \beta H_p (T_{p1} - T_{p2})$, where ρ_p is the average density in the primary loop and the β is the expansion coefficient; note that in Eq. 2 the acceleration pressure drop $\Delta P_{acceleration}$ was neglected, and there is also no pressure head provided by the pumps. The terms in Eq. 2 represent the pressure drop in the core, the pressure drop in the CMT heat exchanger and the pressure drop in the pipes around the loop.

For the second loop (intermediate closed water loop), the conservation equations are similar to those of the primary loop:

$$Q = (T_1 - T_2) \cdot W \cdot C_p \tag{3}$$

$$\Delta P(W) = \Delta P_{friction}(W) + \Delta P_{form}(W) + \Delta P_{gravity}(W) = 0 \tag{4}$$

where Q is the heat removed by each pipe in the ultimate heat exchanger, that is, $Q = Q_p / NN$, and NN is the number of heat exchanger tubes; T_1 and T_2 are the outlet and inlet temperature of the ultimate heat exchanger, respectively; W is the flow rate in each ultimate heat exchanger tube; similar to the primary loop, ΔP is the total pressure drop composed of the friction pressure drop, the form pressure drop and the gravity pressure drop which is $\rho_{\text{int}} g\beta H(T_1 - T_2)$ and ρ_{int} is the average density in the intermediate loop .

The third loop is the seawater flowing through the ultimate heat exchanger. The heat exchanger is immersed in seawater, thus this is an open loop.

Equations describing the heat transfer within each heat exchanger must also be provided. For example, for the heat exchanger in the CMT:

$$Q_{cmt} = h_{cmt} A_{cmt} \Delta T_a \tag{5}$$

$$\Delta T_a = Q_{cmt} \left(\frac{1}{A_{cmt} h_{11}(T_{p1}, T_{p1}, T_{wall1})} + \frac{1}{2\pi\lambda L_1} In(1 + \frac{2\delta}{D}) + \frac{1}{A_{cmt} h_{12}(T_1, T_2, T_{wall2},)} \right) \tag{6}$$

where Q_{cmt} is the heat removed from each pipe in the CMT heat exchanger, that is, $Q_{cmt} = Q_p / N_{cmt}$, and N_{cmt} is the number of tubes in the CMT heat exchanger, fixed at 50. A_{cmt} is the heat transfer area in the CMT heat exchanger, expressed as $2\pi N_{cmt} D L_1$, where L_1 is the length of a tube in the CMT (fixed at 6 m) and D is the tube diameter (fixed at 0.05 m); the T_{wall1} and T_{wall2} are the wall temperature of the primary and intermediate side. ΔT_a is the logarithmic mean temperature difference between the fluids in primary and intermediate loop, defined as $\Delta T_a = \left(T_{p1} - T_{p2} + T_1 - T_2\right) / In \frac{T_{p1} - T_2}{T_{p2} - T_1}$; h_{cmt} is the overall heat transfer coefficient for the heat exchanger, which can be divided into three thermal resistances in series: the convection heat transfer on the primary side, conduction through the pipe wall, and again convection on the intermediate loop side. The heat transfer coefficients h_{11} and h_{12} , can be found from forced or - natural convection correlations depending on the ratio of the Grashof Number to the square of the Reynolds number Gr / Re^2. In Eq(6) δ is the thickness of the pipe wall, λ is the thermal conductivity of the tube wall.

An analogous equation for the logarithmic mean temperature difference between the intermediate loop and the sea water , ΔT_b , applies to the ultimate heat exchanger:

$$Q = h_{sea} A_{sea} \Delta T_b \tag{7}$$

$$\Delta T_{\mathrm{b}} = Q\left(\frac{1}{A_{sea} h_{21(T_1, T_1, T_{wall3})}} + \frac{1}{2\pi\lambda L_2} In(1+\frac{2\delta}{D}) + \frac{1}{A_{sea} h_{22(T_{sea}, T_{wall4},)}} \right), \tag{8}$$

where h_{sea} is the overall heat transfer coefficient for the heat exchanger of seaside; A_{sea} is the ultimate heat exchanger area; ΔT_b is the logarithmic mean temperature difference between the intermediate loop and the sea; L_2 is the pipe length; h_{21} and h_{22} are the heat transfer coefficient for the intermediate side and sea side, respectively; the T_{wall3} and T_{wall4} are the wall temperature of the intermediate and sea side in the ultimate heat exchanger

The ultimate heat exchanger area A_{sea} is

$$A_{sea} = \pi \cdot NN \cdot D \cdot L_2 , \tag{9}$$

where *NN* and *D* have been fixed based on engineering judgment (*NN* is set to 50 and *D* is set to 0.05 m), however, L_2 must be found.

Consider all the equations and unknowns above: there are nine equations and seven unknowns, namely, A_{sea}, L_2, T_{p2}, W_p, W, T_1, T_2, ΔT_a and ΔT_{b}., we can therefore obtain the length of the heat exchanger L_2 by iteration calculation (Fig. 5).

The hand-calculation results are reported in Table II along with the predictions of a RELAP5 model whose nodalization diagram is shown in Fig. 6. This model includes the core, pumps, pressurizer, steam generator, steam drum, core makeup tanks and DRACS; it features 514 nodes; the core is modeled as one average channel equivalent to 23496 actual channels (the product of the number of assembly, 89, and the number of channels per assembly, 264); the boundary conditions are adiabatic for the steam generator heat exchanger and the incoming sea water is assumed to be at fixed temperature, as 20 ℃. For the same steady-state conditions and inputs, there is a reasonable agreement between the hand calculations and RELAP5. However, the RELAP5 prediction for heat exchanger is somewhat higher, probably due to differences in the heat transfer coefficient and friction factor correlations used in the two analyses. Therefore we conservatively adopted the RELAP5-predicted heat exchanger height of 3.5 m.

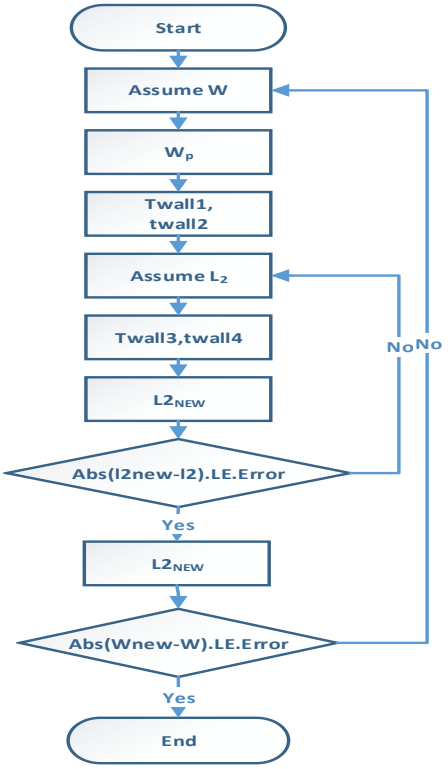

Fig 5. Flow chart of the hand calculations for the DRACS sizing

Table II. Results from RELAP5 and hand calculations for the same primary conditions

	Reactor power (MWt)	Primary pressure (MPa)	Temperature of CMT (K)	Flow Rate of the primary loop (kg/s)	Flow Rate of the intermediate loop (kg/s)	Height of the heat exchanger (m)
RELAP5	10.3	5.9	487.5	29.0	66.0	3.5
Hand calculations	10.3	5.9	487.5	31.7	53.	2.8

4. Performance of the DRACS

RELAP5 is employed to analyze the performance of the DRACS during a station blackout, to ensure that the standard safety limits reported in Table III are respected with acceptable margin.

Table III. Postulated safety limits for the station blackout event in the OFNP-300

Parameter	Limit value
Peak Cladding Temperature (PCT)	1200℃
Max temp. UO2	< melting point (2800°C)
Minimum Departure from Nucleate Boiling Ratio (MDNBR)	> 1.3
Reactor Coolant System (RCS) pressure	< 19 MPa (RPV design pressure)
Core outlet temp	Below saturation (only for LOFA)

An initial period of 200 s of full power operation is simulated to achieve nominal steady-state conditions. The blackout accident is simulated as follows: all the pumps stop at t=200 s and coast down until all forced flow is completely lost. The scram ("S") signal is activated 3 seconds after the pumps stop; the feedwater and main steam isolation valves are closed at the "S" signal; the CMTs start to inject at the low pressure signal (<11.7MPa).

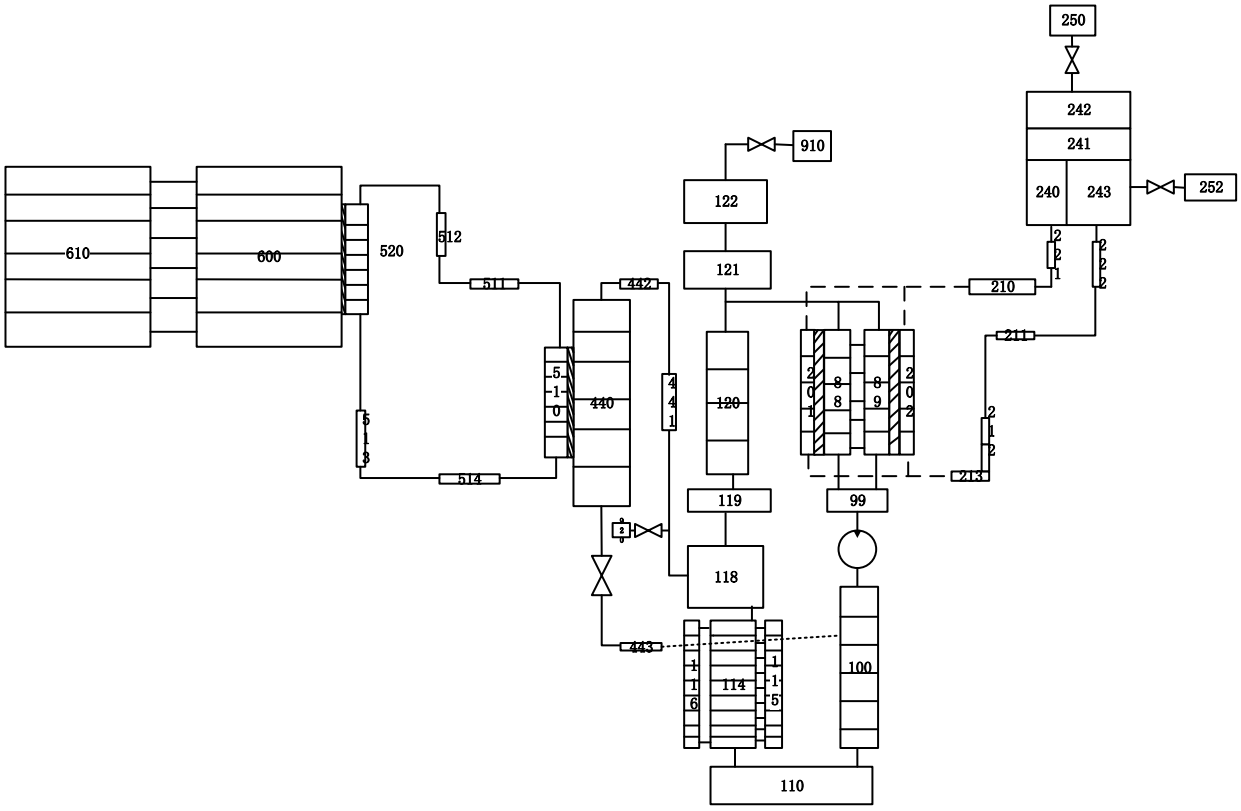

Fig 6. RELAP5 nodalization diagram for OFNP-300

Fly wheels are installed on the reactor coolant pumps, to extend the coast down period. The effect of the moment of inertia of the pumps is significant during the first few seconds of the station blackout. The MDNBR history for various values of the pump moment of inertia is shown in Fig. 7. It can be seen that for a moment of inertia of 1000.0 lb·ft^2 (42.14 kg·m^2), the MDNBR remains well above the safety limit.Thus this value was used in the following analysis. To provide a larger moment of inertia in a smaller space, a uranium alloy could be used for the fly wheels material, and the diameter would be about half that of the AP1000 reactor coolant pump flywheels.

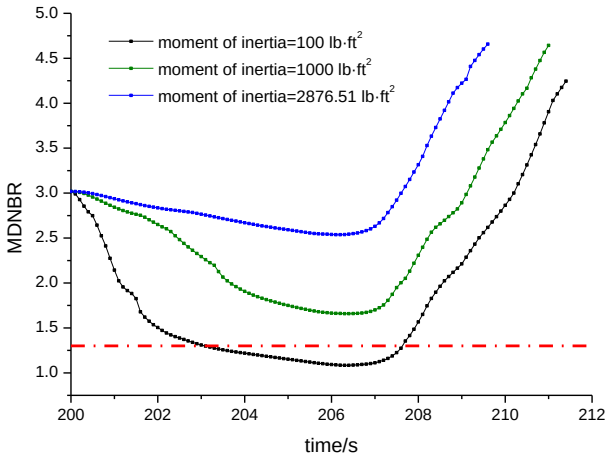

Fig 7. MDNBR during the early stages of the OFNP300 station blackout event, for various values of the pump moment of inertia.

The reactor power, coolant pressure, core temperatures and flow rate during the station blackout are shown in Figures 8, 9, 10 and 11, respectively. At the beginning of the accident, the primary flow rate decreases quickly due to the pump trip. Heat produced by the core cannot be removed effectively by the coolant, thus the temperature of the primary loop increases, leading to the increase in pressure (Fig. 9). When the reactor trips soon after the pump trip, the power drops rapidly (Fig. 8). Thus the pressure and temperatures drop as well. In the long term (time>3000s), the pressure and temperature remain relatively constant as the DRACS removes all the decay heat from the core. The sudden increase in flow rate (Fig.11), and the corresponding drop of the core temperatures at about 250s (Fig. 10) are due to the flow injection from the CMT. As shown in Fig. 11, the flow rate does not drop to zero immediately due to pump coast down, and natural circulation subsequently sets in. Note that the pressure and subcooling limits are not violated throughout the event.

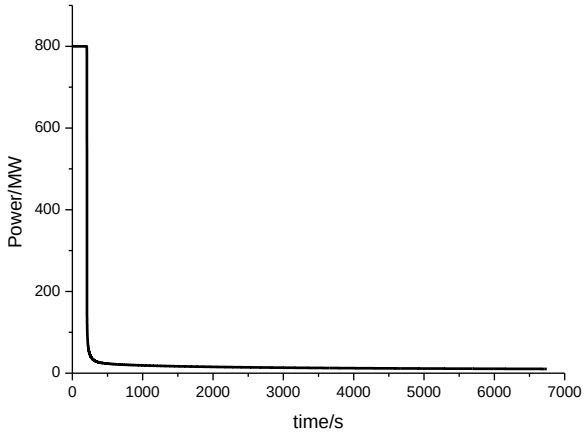

Fig 8. Reactor power during the OFNP-300 station blackout

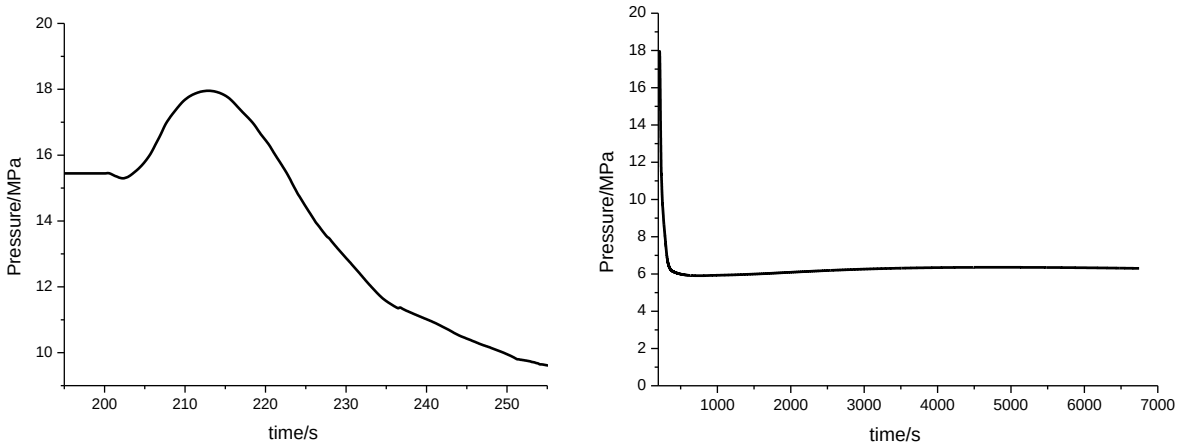

Fig 9. Reactor coolant pressure during (a) the early stages and (b) long term of the OFNP-300 station blackout

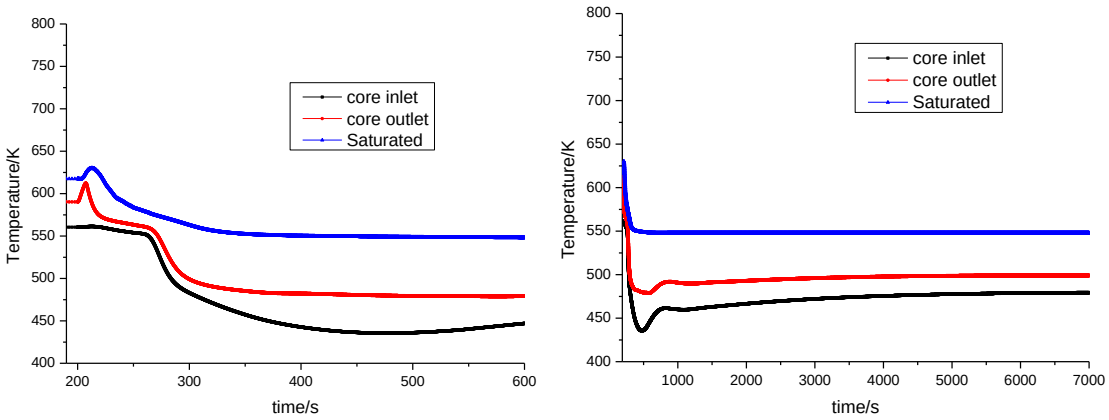

Fig 10. Core temperatures during (a) the early stages and (b) long term of the OFNP-300 station blackout

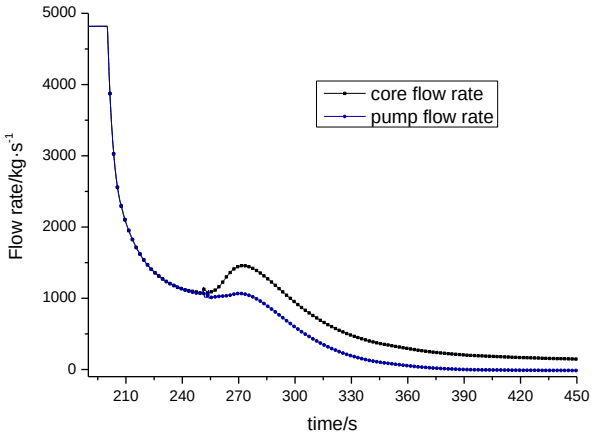

Fig 11. Core flow rate and pump flow rate during the early stages of the OFNP-300 station blackout

The flow rate and temperature of the DRACS intermediate water loop are illustrated in Fig. 12 and Fig. 13, respectively. The flow rate increases rapidly at first as the CMT injects and the DRACS intermediate loop receives a great amount of heat from the primary loop. The flow rate and temperature finally approach a quasi-steady state, confirming the ability of the DRACS to remove residual heat from the core by natural circulation. The input heat power from the primary loop and output into the seawater are shown in Fig. 14. The output power is initially very low because the intermediate loop temperature is initially closed to the seawater temperature. After a period during which the intermediate loop temperatures and the natural circulation flow rate have grown, the input and output powers of the intermediate loop are finally balanced and hence a quasi-steady state is achieved.

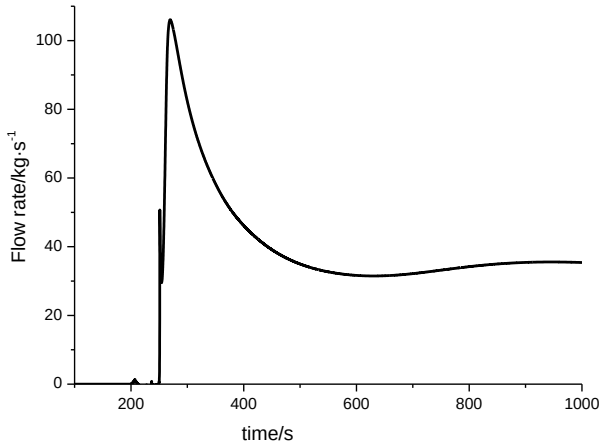

Fig 12. DRACS flow rate during the OFNP-300 station blackout

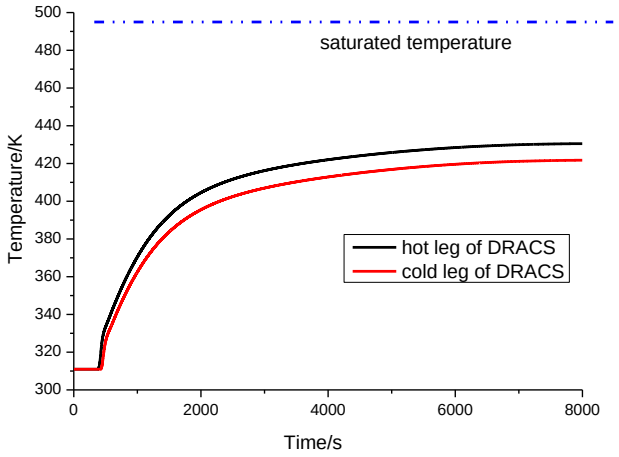

Fig 13. DRACS temperatures during the OFNP-300 station blackout

Figures 15 and 16 show the seawater temperatures and flow rate in the ultimate heat exchanger, respectively. Seawater temperature keeps rising moderately since the start of the natural circulation, and no bulk boiling occurs. Seawater supply is available indefinitely, therefore the ultimate heat sink is never lost in the OFNP design.

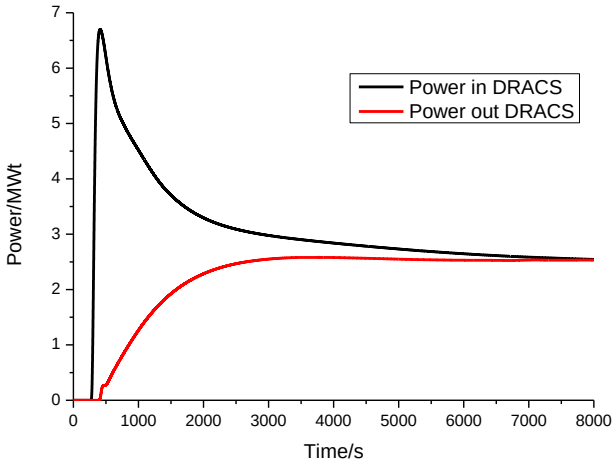

Fig 14. DRACS power input and output during the OFNP-300 station blackout

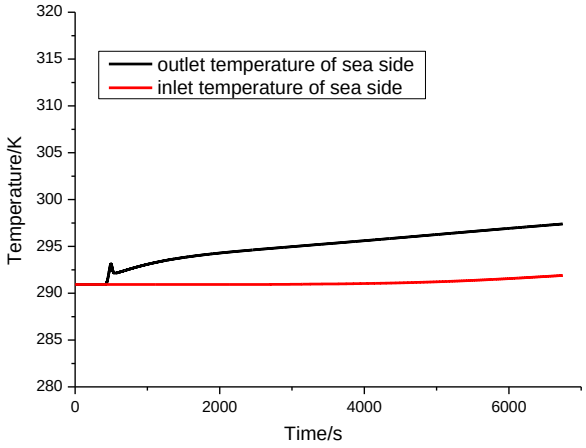

Fig 15. Seawater temperature in the ultimate heat exchanger during the OFNP-300 station blackout

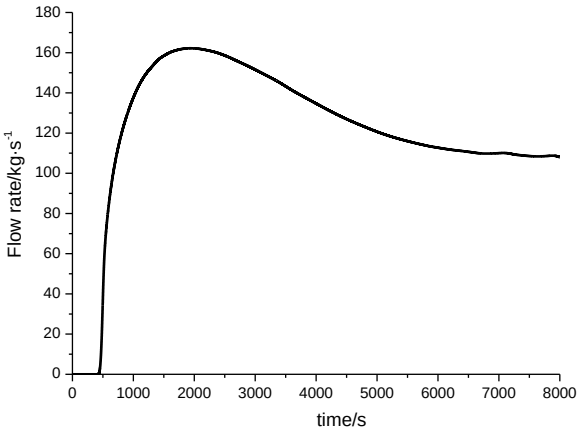

Fig 16. Seawater flow rate in the ultimate heat exchanger during the OFNP-300 station blackout.

5. CONCLUSIONS

The design and performance of the ocean-based Direct Reactor Auxiliary Cooling System (DRACS) for the 300-MWe version of the OFNP was presented. The DRACS is designed to remove the residual heat during a station blackout or other abnormal event in which the reactor coolant system does not depressurize. The DRACS ultimate heat exchanger height was selected to be 3.5 m, based on hand calculations and RELAP5 estimates. The RELAP5 analysis suggests that the reactor coolant pressure and subcooling limits are satisfied during the station blackout. The MDNBR limit is also met if the flywheel for the reactor coolant pumps is sized to ensure a sufficiently slow coast down of the pumps in the early stages of the station blackout. Future work will include analysis of other Design Basis Events (DBE), such as the loss of coolant accident, for both OFNP-300 and OFNP-1100, as well Beyond Design Basis Events (BDBE).

ACKNOWLEDGMENTS

The author Jing Zhang is thankful for the financial support from the China Scholarship Council (CSC) and the support from Xi'an Jiaotong University. This project is funded by the MIT Research Support Committee.

REFERENCES

1. J. Buongiorno, J. Jurewicz, M. Golay, N. Todreas, "Light-Water Reactors on Offshore Floating Platforms: Scalable and Economic Nuclear Energy", Paper 15366, Proceedings of ICAPP '15, Nice, France, May 3-6, (2015).
2. M.J. Memmott, A.W. Harkness, J. VAN WYK,"Westinghouse Small Modular Reactor nuclear steam supply system design", Proceedings of the 2012 International Congress on Advances in Nuclear Power Plants-ICAPP'12, 2012,2, 973-983 (2012).
3. M.J. Memmott, C. Stansbury, C. Taylor,"Westinghouse Small Modular Reactor Balance of Plant and Supporting Systems Design", Proceedings of the 2012 International Congress on Advances in Nuclear Power Plants-ICAPP'12, (2012).
4. J.M. Cronje, J.J. Van Wyk, M.J. Memmott,"Overview of the Westinghouse Small Modular Reactor Building Layout", Proceedings of the 2012 International Congress on Advances in Nuclear Power Plants-ICAPP'12, (2012).
5. M.C. Smith, R.F. Wright,"Westinghouse Small Modular Reactor Passive Safety System Response to Postulated Events", Proceedings of the 2012 International Congress on Advances in Nuclear Power Plants-ICAPP'12, (2012).
6. J. Jurewicz, J. Buongiorno, N. Todreas, M. Golay "Conceptual Design of an Offshore Floating Nuclear Power Plant with Spar-Type Platform", Paper 1104, The 10th International Topical Meeting on Nuclear Thermal-Hydraulics, Operation and Safety (NUTHOS-10), Okinawa, Japan, Dec. 14-18, (2014).

Nomenclature

Q : power through each ultimate heat exchanger tube	Q_{cmt} : power through each CMT heat exchanger tube
Q_s : total residual power	Q_p : power through each CMT
T_{p1} : core outlet temperature	T_{p2} : core inlet temperature
T_1 : ultimate heat exchanger outlet temperature	T_2 : ultimate heat exchanger inlet temperature
T_{wall1} : wall temperature of primary side in CMT heat exchanger	T_{wall2} : wall temperature of intermediate loop in CMT heat exchanger
T_{wall3} : wall temperature of intermediate loop in ultimate heat exchanger	T_{wall4} : wall temperature of sea side in ultimate heat exchanger
ΔT_a : logarithmic mean temperature difference between primary and intermediate loop	ΔT_b : logarithmic mean temperature difference between intermediate loop and sea side
W_P : flow rate in each CMT heat exchanger tube	W : flow rate in each ultimate heat exchanger tube
ΔP : total pressure drop of intermediate loop	ΔP_p : total pressure drop of primary loop
$\Delta P_{fiction}$: friction pressure drop	$\Delta P_{gravity}$: gravity pressure drop
$\Delta P_{acceleration}$: acceleration pressure drop	ΔP_{form} : form pressure drop
h_{cmt} : overall heat transfer coefficient of CMT heat exchanger	h_{sea} : overall heat transfer coefficient in ultimate heat exchanger
h_{11} : CMT heat transfer coefficient of primary side	h_{12} : CMT heat transfer coefficient of intermediate side
h_{21} : ultimate heat transfer coefficient of intermediate loop	h_{22} : ultimate heat transfer coefficient of sea side
NN : number of tubes in ultimate heat exchanger	N_{cmt} : number of tubes in CMT heat exchanger
L_1 : tube length of CMT heat exchanger	L_2 : tube length of ultimate heat exchanger
A_{cmt} : heat transfer area of CMT heat exchanger	A_{sea} : heat transfer area of ultimate heat exchanger
β : expansion coefficient	λ : thermal conductivity
ρ_p : average density of primary loop	ρ_{int} : average density of intermediate loop
D : tube diameter	δ : thickness of tube wall
C_p : Specific heat capacity	